Title

Light-Patterned RNA Interference of 3D-Cultured Human Embryonic Stem Cells.

Journal

Advanced materials (Deerfield Beach, Fla.), 28(48)

ISSN

0935-9648

Authors

Huang, Xiao

Hu, Qirui

Lai, Yifan

et al.

Publication Date

2016-12-01

DOI

10.1002/adma.201603318

Peer reviewed

Light-Patterned RNA Interference of 3D-Cultured Human Embryonic Stem Cells

*Xiao Huang, Qirui Hu, Yifan Lai, Demosthenes P. Morales, Dennis O. Clegg, and Norbert O. Reich**

Biological processes are stimulated by various molecular and physical signals orchestrated in space and time.[1–4] Tissue and organ generation in vitro for transplant therapy and disease modeling for drug screening[5] are especially demanding for precise control over 3D patterning of different cell types.[2,4,6,7] Advances in this area include the controlled differentiation of pluripotent or multipotent stem cells cultured in 3D matrices followed by self-organization into tissues in vitro.[1,8–11] However, current methods for organoid formation have insufficient control over the course of the morphogenetic processes and the resulting structures inadequately replicate native tissues.[2,4] Microfluidic and nanotopographic patterning approaches establish some organ-level functions ex vivo, but lack the dimensionality to approximate developing tissues.[2,12–14] Light is an ideal stimulus for perturbing the spatiotemporal dynamics of signals in living cells and organisms with high resolution.[15–17] The light-based optogenetic field has answered real biological questions[16] and developed tools for light-controlled genome editing and gene transfection.[18–22] However, these approaches rely largely on the visible light excitation sources and the construction of complex protein fusions via viral transfection. Other alternatives use photocaged small molecules and biopolymers for light-dependent gene regulation,[4,15,23–26] which are limited by cellular delivery hurdles and the use of low tissue-penetrating UV–vis light.[15–17]

We have developed a novel pulsed near-infrared (NIR) light based technique for the spatiotemporal control of gene silencing in 3D-cultured human embryonic stem cells (hESCs) by RNA interference. NIR light can be tightly focused three-dimensionally (down to ≈1 fL)[27] and reach deep through tissues (up to 10 cm).[28,29] Small interfering RNAs (siRNAs) with thiol- modification are covalently attached to hollow gold nanoshells (HGNs) via quasicovalent Au—S bonds,[30–32] followed by the functionalization of a cell-penetrating transactivating transcriptional activator (TAT) peptide.[33] Upon endosomal uptake, NIR light irradiation releases the RNAs from the HGN surface and facilitates endosomal release[34] to initiate gene silencing activity, with no detectable cell damage. We previously demonstrated the high efficiency of siRNA delivery and the biocompatibility of this strategy to human embryonic stem cells.[33] Here, we sought to use the light-controlled siRNA delivery to control individual cells within 3D-cultured hESC "spheroids," utilizing a commonly available two-photon microscope to focus the NIR laser three-dimensionally for excitation.

The two-photon microscope equipped (Olympus Fluoview 1000 MPE) with scan head positioning provides a high resolution spatial control of NIR laser irradiation. Quasar570 labels on siRNA molecules densely assembled on HGNs showed an exquisite pattern of brighter and diffuse fluorescent signals upon irradiation in the selected areas (**Figure 1**a), indicating the light-dependent spatial control of siRNA release.

HGN-transfected hESCs were switched into a synthetic thermoreversible hydrogel (Mebiol Gel, Cosmo Bio Co.) for 3D culture[35] and laser-selected gene silencing. However, only a small fraction of the cells survived. Shortening the HGN incubation time resulted in decreased internalization (data not shown). We tested the addition of Rho-associated proten kinase (ROCK) inhibitor during the HGN incubation (Figure S1a, Supporting Information)[35] and found this treatment significantly increased cell viability in the 3D matrix without detectable changes in HGN internalization (Figure S1b,c, Supporting Information). We also observed that dissociated single cells aggregate into cell clusters with ROCK inhibitor treatment in suspension (Figure S1c, Supporting Information), forming cellular spheroids within 3 d in the 3D matrix. Cell clusters were mixed with the hydrogel and solidified at 37 °C as a thin layer (100–150 μm thick) on grid-bottomed culture dishes (Ibidi) for cell tracking.

The two-photon microscope (adjusted at 800 nm) was used to focus the laser at selected *x*, *y*, and *z* regions of cell clusters to induce siRNA release (Figure 1b). In Figure 1c, red puncta (Quasar570 labeled on siRNA) in the irradiated areas are brighter and more diffuse than neighboring unirradiated areas, indicating spatial control of siRNA release in selected cells guided by the *x*, *y*, and *z* laser scanning from the two-photon microscope.

2D-cultured HeLa cells transduced with green fluorescent protein (GFP) gene were used to optimize the laser irradiation treatment, and we found that laser at 3% of the maximum power (≈2 mW) releases insufficient siRNA, whereas a power of 8% causes some immediate changes in cell morphology (Figure S2, Supporting Information). NIR laser irradiation was performed through *z*-stacks of the cell mass with 1.4 μm intervals, and each *z*-stack (512 × 512 pixels) was scanned line-by-line

Dr. X. Huang, Y. Lai, D. P. Morales, Prof. N. O. Reich
Department of Chemistry and Biochemistry
University of California
Santa Barbara, CA 93106, USA
E-mail: reich@chem.ucsb.edu
Dr. Q. Hu, Prof. D. O. Clegg
Center for Stem Cell Biology and Engineering
Department of Molecular, Cellular, and Developmental Biology
University of California
Santa Barbara, CA 93106, USA

DOI: 10.1002/adma.201603318

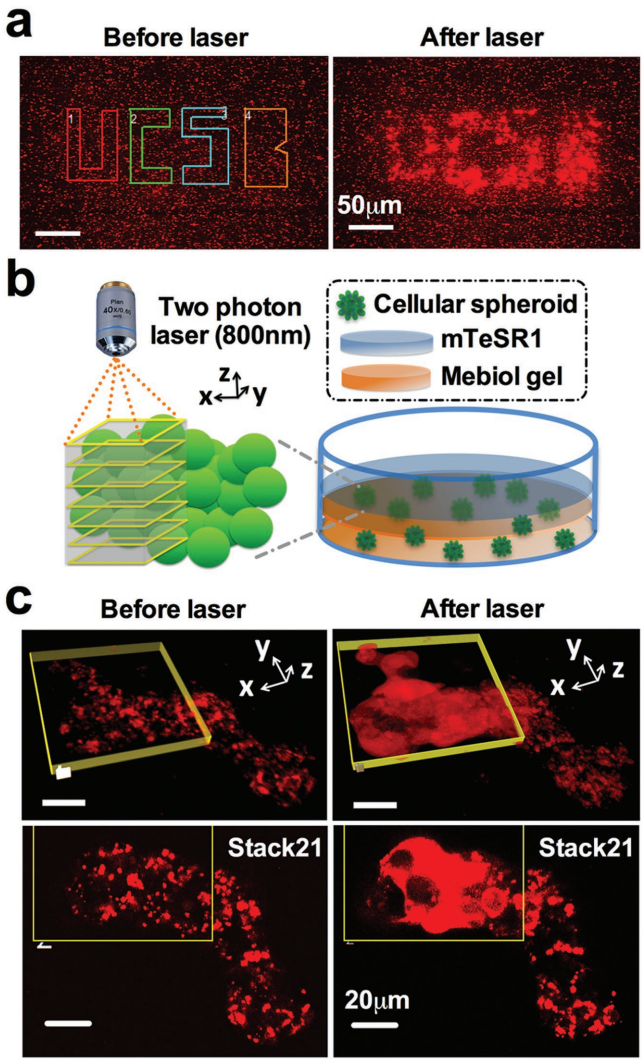

Figure 1. Spatially controlled siRNA delivery in 3D-cultured hESCs. a) NIR laser patterned siRNA release (in frames) on a cell-free glass slide. b) Schematic of siRNA delivery in selected 3D-cultured hESCs using a two-photon microscope. c) Laser controlled siRNA release (in yellow frame) within one cell cluster in a 3D matrix. Top panel: 3D side view of 43 *Z*-stacks; bottom panel: Stack 21. Red: Quasar570 labeled on siRNA.

(2 μs per selected pixel, 5% of the maximum power), a total of five times. hESC H9 cells were then transduced with the GFP gene and cultured in the 3D hydrogel after HGN transfection. Laser irradiation of hESC H9 cell clusters in the hydrogel stimulated the release of siRNA indicated by the bright and diffuse red puncta (Quasar570 on siRNA), with minimum damage to the GFP signal (**Figure 2**a). 3 d later, the clusters exposed to the laser were imaged (Figure 2b), and quantified the fluorescence (Figure 2c). Laser-treated spheroids showed ≈65% less GFP expression on average compared to the nonirradiated controls (Figure 2c).

Importantly, cells irradiated with the NIR laser grew at the same rate as cells without laser treatment, assessed by the 3D volume analysis (Figure S3, Supporting Information). HGN mediated GFP-siRNA delivery to mCherry cotransduced H9 cells resulted in selective GFP knockdown without any detectable changes in mCherry expression (Figure S4, Supporting Information), further confirming the specificity of GFP knockdown and the unchanged cell viability after laser irradiation. Markers for cell pluripotency were also probed by immunocytochemistry of cells treated with HGNs and an equivalent NIR laser (femtosecond Ti:sapphire regenerative amplifier, 130 fs pulse duration, 1 KHz repetition rate) with a ≈4 mm beam diameter covering the entire 3D hydrogel. Similar levels of OCT3/4 and TRA-1-60 were observed in cells treated with HGNs and laser compared to the control without laser treatment (Figure S5, Supporting Information). Based on these results, this approach is highly biocompatible.

NIR laser activation of a subpopulation of cells within one cell cluster provides unprecedented spatial control. Interestingly, although the spheroids retained a similar shape 3 d after laser treatment, GFP fluorescence showed different patterns of downregulation: edged, mosaic, and retrograde (**Figure 3**a). In contrast, the downregulation of GFP-transduced HeLa cells loaded with HGNs and irradiated on a 2D culture dish did not show distinct patterns (Figure 3b). This suggests that undifferentiated H9 cells migrate[36] within the spheroid, and neither laser irradiation nor siRNA release alters this migration.

The timing of siRNA activation can also be tuned by laser irradiation. Cellular spheroids were irradiated with NIR laser 2 h (Day 0), 1 d, 2 d, and 3 d post HGN incubation and 3D hydrogel placement. Functionalized HGNs exhibited laser-dependent release of functional siRNA up to 2 d after cellular uptake, while no siRNA knockdown of GFP was observed when the time lag extended to 3 d (**Figure 4**a,b). Consistently, the siRNA signal (by Quasar570 fluorescence) in the 3D-cultured H9 cells dramatically drops 2 d after particle incubation (Figure S6, Supporting Information), indicating the dilution or degradation of siRNA in cells. We carried out similar experiments with HeLa cells transduced with GFP (≈24 h doubling time)[37] to explore why gene silencing is lost after 3 d in hESC. However, laser irradiation 3 d post HGN internalization still showed effective gene silencing (Figure 4c and Figure S7 (Supporting Information)), indicating loss of siRNA knockdown is likely due to rapid siRNA degradation in hESCs rather than dilution by cell division.

We also investigated the stability of siRNA coated HGNs in buffer, with or without the exposure to glutathione (GSH), the main reducing agent in cells. We found that the siRNA protected by HGNs remain intact at neutral pH for at least a month, whereas overnight exposure to GSH at 0.01×10^{-3} M releases half of the loading (Figure S8, Supporting Information). However, the siRNA-HGN constructs accumulate in the endosome[38] and endosomal GSH levels are quite low.[39] Furthermore, release of siRNA from the endosome requires laser exposure, as shown by the unchanged GFP expression in both hESC and HeLa cells 6 d post siRNA coated HGN internalization (Figure 4 and Figure S7 (Supporting Information)). This provides the basis for the spatial control of siRNA release over time.

We also tested an alternative HGN transfection approach by treating hESCs as they develop from single cells to spheroids in 3D culture. Fresh medium containing HGNs were fed to gel-encapsulated cells every day to overcome any inefficiency of

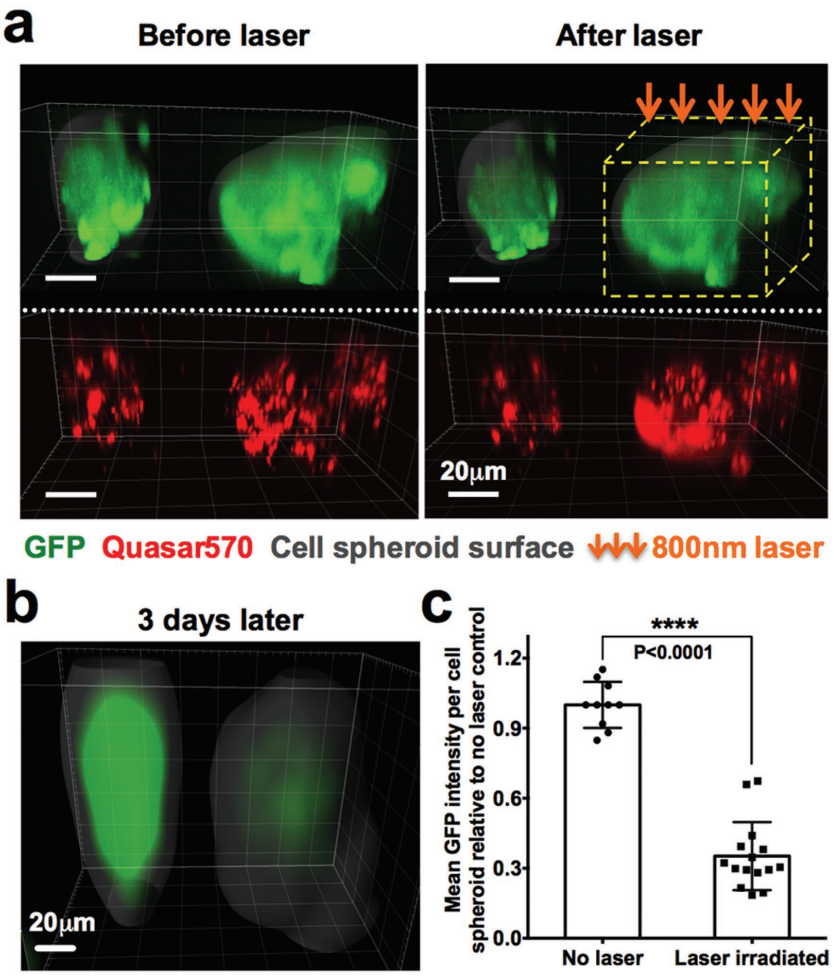

Figure 2. GFP gene knockdown of 3D-cultured hESC H9 cell clusters by NIR light irradiation. a) Confocal fluorescence microscopy (in single-photon mode) of H9-GFP clusters before and after 800 nm laser irradiation (in two-photon mode) compared to nonirradiated control cluster. b) Fluorescence imaging of the same H9-GFP spheroids shown in (a) 3 d post laser irradiation. c) Averaged GFP intensity of spheroids (3D pixel intensity analysis) 3 d post laser treatment.

HGN penetration into the spheroids. As a result, HGNs distributed equally across the whole body of cellular spheroids generated in the thin hydrogel layer (Figure S9, Supporting Information). Although we relied largely on transfecting HGNs prior to 3D casting, the alternative method clearly has advantages such as the temporal control of gene silencing in a longer time window.

In summary, we have developed a novel approach to regulate genes in human embryonic stem cells in a 3D matrix with unprecedented spatiotemporal control. We demonstrated 3D siRNA release and gene silencing in selected cells upon laser irradiation. This approach is viable for 2 d after HGN treatment, providing a basis for spatiotemporal control of gene regulation in stem cells for in vitro organogenesis. We are currently applying this technology to generate an in vitro optic cup for retinal tissue growth by spatial control of Wnt signaling to pattern the differentiation of hESC to neural retina and retinal pigment epithelium.[11,40] Moreover, the two photon excitation approach can also be combined with in vivo imaging[41] to become a promising means for investigation of developmental processes in vivo.

Experimental Section

2D Cell Culture: The hESC including H9 (passage 60–70, WiCell Research Institute), transduced H9-GFP (passage 65–75), and H9-GFP/mCherry (passage 75–85) were maintained on Matrigel (BD Biosciences) coated plates (BD Falcon) in mTeSR1 medium (Stem Cell Technologies) at 37 °C in 5% CO_2 atmosphere. Cells were passaged by nonenzymatic manual dissection every 5–7 d. HeLa (ATCC) and HEK293T cells were cultured in Dulbecco's Modified Eagle Medium (DMEM, Hyclone) supplemented with 10% fetal bovine serum (FBS, Hyclone). Cell culture medium was supplemented with 50 μg mL^{-1} Normocin (InvivoGen).

Lentiviral Transduction: The generation of transduced H9-GFP, H9-GFP/mCherry, and HeLa-GFP cell lines through lentiviral transfection is described in the Supporting Information.

hESC H9 Cell Culture in 3D Hydrogel: Each well of 2D cultured hESCs on 6-well plates was dissociated by incubating with 500 μL Phosphate-buffered saline (PBS, Ca^{2+} and Mg^{2+} free, Invitrogen #10010-023) at 37 °C in a 5% CO_2 atmosphere for 10 min followed by manual dissection to suspend the cells. The suspended cell aggregate solution was added to 1 mL mTeSR1 and pipetted gently 10–15 times with a P1000 pipette to further decrease the size of the cell aggregates (approximately most optimal with 5–10 cells per aggregate). Thereafter, ≈4×10^5 cells in single cell or small cell aggregates were mixed with 200 μL Poly(N-isopropylacrylamide) (PNIPAAm)-Polyethylene (PEG) (Mebiol Thermoreversible Hydrogel, Cosmo Bio) and dissolved in E8 medium (Stem Cell Technologies) at 4 °C using a positive-displacement pipette (Microman M250, Gilson). Then, 100 μL of homogenized cell solution was transferred onto the grid area of an ice-chilled petri dish (μ-Dish$^{35\ mm}$ Grid-500, Ibidi) to cover the whole surface as a thin layer of liquid (≈100–150 μm), followed by incubation at 37 °C for 5 min to solidify the hydrogel. 3 mL of warm E8 medium containing 10×10^{-6} M ROCK inhibitor (Stem Cell Technologies, Y-27632) was then added on top of the hydrogel and refreshed every day during the subsequent 3D culture step. To collect cells from the 3D hydrogel, 1 mL ice-cold PBS was placed on the hydrogel layer and incubated at 4 °C for 5 min to dissolve the hydrogel, followed by centrifugation at 145 × *g* for 3 min.

HGN Synthesis and the Assembly of siRNA and TAT Peptide: The protocols for HGN synthesis and the assembly of siRNA (Table S1, Supporting Information) and TAT peptide are described in the Supporting Information.

Nanoparticle Transfection Protocols: Cells were transfected with particles in suspension prior to hydrogel embedment to achieve efficient internalization of nanoparticles throughout the cell clusters in 3D culture. Cells were suspended on 6-well plates and dissociated into single cells or small cell aggregates using PBS (Ca^{2+} and Mg^{2+} free) as described above. Cells were centrifuged at 145 × *g* and resuspended in 200 μL transfection medium (mTeSR1 + 10% FBS + 10×10^{-6} M ROCK inhibitor + 13×10^{-12} M HGNs) at ≈2×10^6 cells per mL, followed by 37 °C and 5% CO_2 incubation for 2 h with gentle pipetting of the solution five times every 30 min. Thereafter, cells were washed by adding 1.2 mL cold PBS and centrifuging at 55 × *g* for 3 min, followed by resuspending

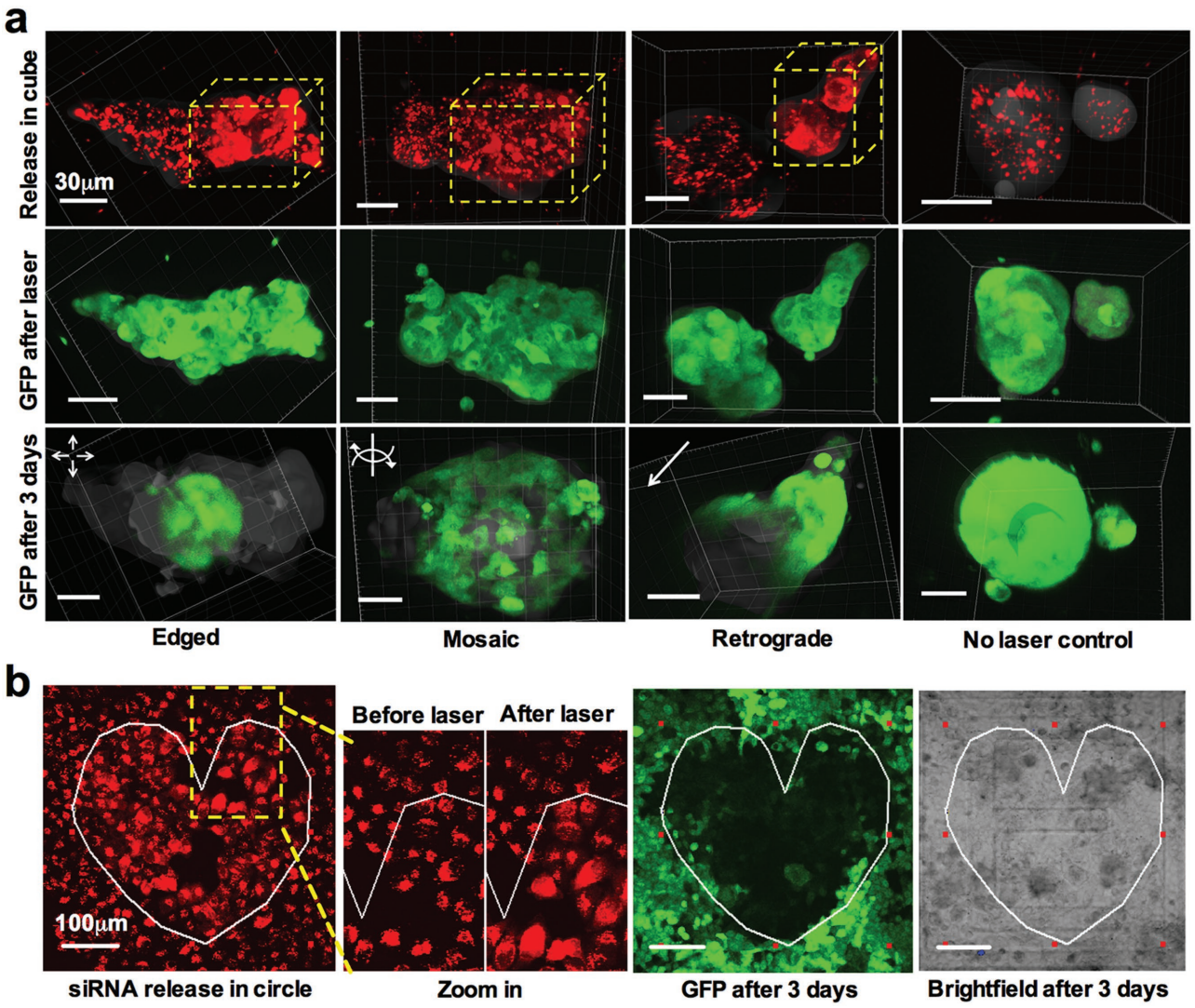

Figure 3. GFP downregulation patterns of 3D-cultured hESCs and 2D-cultured HeLa cells 3 d after spatially controlled siRNA release. a) 3D-cultured H9 spheroids with a subpopulation of cells treated with GFP-siRNA show different GFP downregulation patterns 3 d later: edged, mosaic, and retrograde. Top panel: Cells within the yellow dashed line cubes are irradiated with laser; Middle and Bottom panel: GFP fluorescence images of cellular spheroids before and after laser treatment for 3 d. b) 2D-cultured HeLa cells show similar patterns of GFP downregulation 3 d later as outlined by the laser irradiation. siRNA molecules are labeled with Quasar570 dye (red); GFP fluorescence (Green); Cell outline (grey).

in 200 µL ice-cold PNIPAAm-E8 solution. 100 µL of the cell mixture was transferred to the gridded petri dish and solidified at 37 °C for 5 min before the addition of ROCK inhibitor containing medium, as described above.

As an alternative way of particle transfection, dissociated and suspended hESCs from 2D cultures were cast in a thin layer of 3D Mebiol gel on a gridded petri dish as described above, followed by the daily feeding of fresh HGN-containing medium (E8 + 10% FBS + 10×10^{-6} M ROCK inhibitor + 13×10^{-12} M HGNs) for 5 d.

For the transfection of 2D-cultured HeLa-GFP cells, ≈1×10^5 cells were plated on a gridded petri dish, and the next day fresh medium (DMEM + 10% FBS) containing 6.5×10^{-12} M HGNs was added and incubated at 37 °C in 5% CO_2 for 2 h. Cells were then washed twice with fresh medium.

Two-Photon Microscope Excitation and Imaging: To activate the siRNA release, 2D-cultured HeLa cells and 3D-cultured H9 cells on gridded petri dishes post HGN transfection were irradiated with a pulsed NIR laser, generated by a two-photon microscope (Olympus Fluoview 1000 MPE) with environmental chamber adjusted at 30 °C and 5% CO_2 atmosphere. The two-photon microscope was equipped with a 25× water immersion objective (numerical aperture 1.05), a mode-locked titanium-sapphire femtosecond (fs) tunable (690–1020 nm) pulsed laser (100 fs pulse duration, 80 MHz repetition rate, MaiTai HP, Newport-Spectra physics), 473/559/633 nm laser diodes, a transmitted light detection system, and a scan head controlled by Fluoview software. The MaiTai laser was tuned to 800 nm at 5% of the maximum power (≈2 mW) and exposed to *z*-stacks (1.4 µm interval) of intended cell(s) through line-by-line scanning (125 KHz) of selected pixels in each *z*-stack (512 × 512 pixels, 0.331 µm per pixel) at 2 µs per pixel for five repetitions. The sample was imaged in a single-photon confocal mode with the blue (for GFP) and green (for Quasar570 or mCherry) laser diodes at a scan speed of 80 KHz before and after the exposure to the MaiTai fs laser to compare the fluorescence signal difference caused by the laser treatment.

Cell(s) treated with laser or without laser were relocated after 3 d according to the grid information on the bottom of the petri dish,

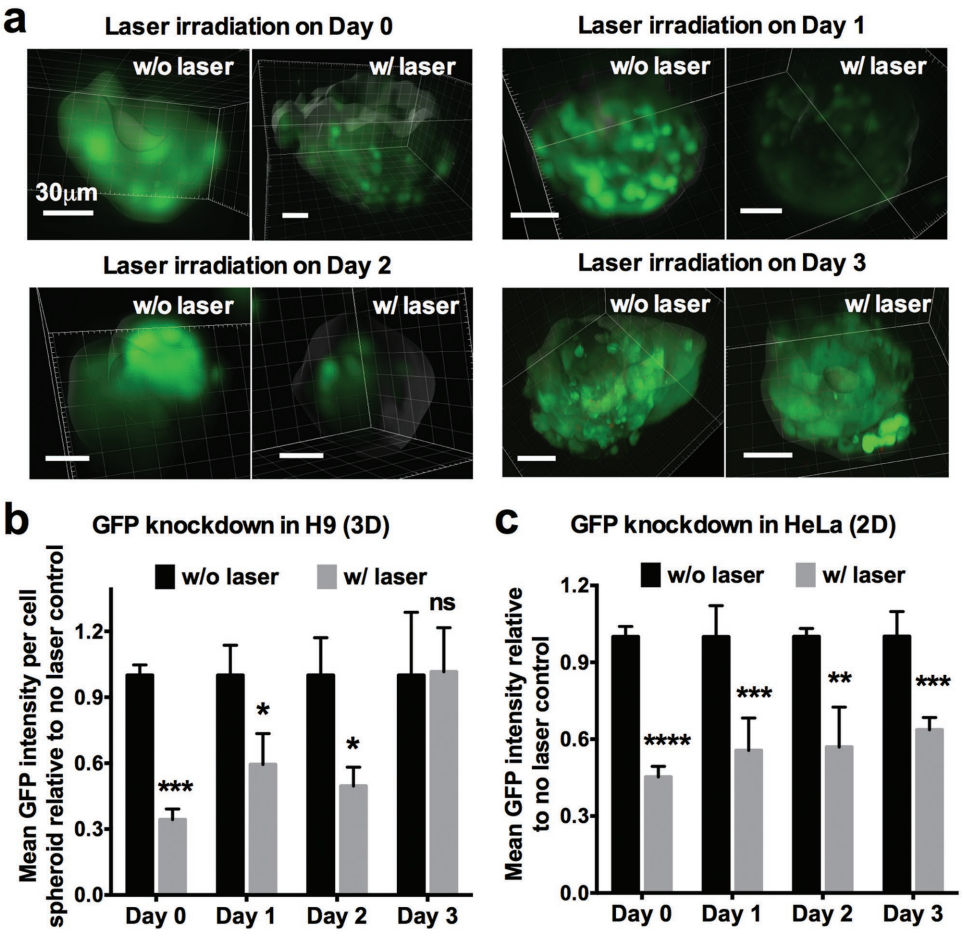

Figure 4. Temporally controlled gene silencing in 3D-cultured H9 cells and 2D-cultured HeLa cells. a) Fluorescence imaging of GFP (green) in 3D-cultured H9 spheroids (grey for cell outline) 3 d post laser irradiation. Cellular spheroids were irradiated with 800 nm laser using the two-photon microscope 2 h (Day 0), 1 d, 2 d, and 3 d after HGN incubation. b) Averaged GFP fluorescence intensity of H9 spheroids in (a) from the 3D green pixel intensity analysis within the cell outline. c) Averaged GFP fluorescence intensity (pixel intensity analysis) of 2D-cultured HeLa cells 3 d post laser irradiation exposed to cells 2 h (Day 0), 1 d, 2 d, and 3 d after particle incubation. *, $p < 0.5$; **, $p < 0.01$; ***, $p < 0.001$; ****, $p < 0.0001$.

and imaged in the single-photon confocal mode for GFP, mCherry, or Quasar570 fluorescence, as well as brightfield images from the transmitted channel.

Image Quantification and Statistical Analysis: 3D images obtained from the single-photon confocal mode of the two-photon microscope were analyzed for the GFP, mCherry, and Quasar570 fluorescence intensity of cellular spheroids using Imaris 8.1 software (Bitplane). The 3D surface of spheroid was modeled according to the brightfield images and the volume was measured as an indication of cell growth. GFP and mCherry fluorescence intensity were averaged by the volume for the comparison of gene silencing effect with and without laser. Images of HeLa cells from the 2D petri dish culture were analyzed for GFP fluorescence intensity using ImageJ software and averaged by the area.

Data with error bars were from at least three replicate experiments and were presented as the mean ± standard deviation. Statistical analyses were done using the statistical package Instat (GraphPad Software), and the means of replicates were evaluated using *t*-tests.

Supporting Information

Supporting Information is available from the Wiley Online Library or from the author.

Acknowledgements

This work was supported by the National Institutes of Health (NIH) grant R01 EB012637 and the California Institute for Regenerative Medicine (CIRM) grant TG2-01151. The authors thank Mary Raven for the help with the two-photon microscopy (supported by the NIH grant S10RR022585) and David Schaffer for the helpful discussion about the stem cell 3D culture protocol. The authors also wish to acknowledge Cassidy Hinman at the UCSB Laboratory for Stem Cell Biology and Engineering, supported by the CIRM grant CL1-00521. X.H. acknowledges support from the Chinese Scholarship Council (CSC) file number 2011674001.

Received: June 23, 2016
Revised: September 15, 2016
Published online: October 27, 2016

[1] Y. Sasai, *Nature* **2013**, *493*, 318.
[2] N. Gjorevski, A. Ranga, M. P. Lutolf, *Development* **2014**, *141*, 1794.
[3] J. L. Carvalho-de-Souza, J. S. Treger, B. Dang, S. B. H. Kent, D. R. Pepperberg, F. Bezanilla, *Neuron* **2015**, *86*, 207.
[4] A. P. McGuigan, S. Javaherian, *Annu. Rev. Biomed. Eng.* **2016**, *18*, 1.

[5] S. Aday, R. Cecchelli, D. Hallier-Vanuxeem, M. P. Dehouck, L. Ferreira, *Trends Biotechnol.* **2016**, *34*, 382.
[6] Y. Sasai, *Cell Stem Cell* **2013**, *12*, 520.
[7] K. Nakao, R. Morita, Y. Saji, K. Ishida, Y. Tomita, M. Ogawa, M. Saitoh, Y. Tomooka, T. Tsuji, *Nat. Methods* **2007**, *4*, 227.
[8] J. R. Spence, C. N. Mayhew, S. A. Rankin, M. F. Kuhar, J. E. Vallance, K. Tolle, E. E. Hoskins, V. V. Kalinichenko, S. I. Wells, A. M. Zorn, N. F. Shroyer, J. M. Wells, *Nature* **2011**, *470*, 105.
[9] M. Eiraku, N. Takata, H. Ishibashi, M. Kawada, E. Sakakura, S. Okuda, K. Sekiguchi, T. Adachi, Y. Sasai, *Nature* **2011**, *472*, 51.
[10] H. Suga, T. Kadoshima, M. Minaguchi, M. Ohgushi, M. Soen, T. Nakano, N. Takata, T. Wataya, K. Muguruma, H. Miyoshi, S. Yonemura, Y. Oiso, Y. Sasai, *Nature* **2011**, *480*, 57.
[11] T. Nakano, S. Ando, N. Takata, M. Kawada, K. Muguruma, K. Sekiguchi, K. Saito, S. Yonemura, M. Eiraku, Y. Sasai, *Cell Stem Cell* **2012**, *10*, 771.
[12] K. Kolind, K. W. Leong, F. Besenbacher, M. Foss, *Biomaterials* **2012**, *33*, 6626.
[13] T. Fujie, X. Shi, S. Ostrovidov, X. Liang, K. Nakajima, Y. Chen, H. Wu, A. Khademhosseini, *Biomaterials* **2015**, *53*, 86.
[14] E. H. Ahn, Y. Kim, K. Gupta, S. S. An, J. Afzal, S. Lee, M. Kwak, K. Y. Suh, D. H. Kim, A. Levchenko, *Biomaterials* **2014**, *35*, 2401.
[15] C. Brieke, F. Rohrbach, A. Gottschalk, G. Mayer, A. Heckel, *Angew. Chem., Int. Ed. Engl.* **2012**, *51*, 8446.
[16] D. Tischer, O. D. Weiner, *Nat. Rev. Mol. Cell Biol.* **2014**, *15*, 551.
[17] A. Deiters, *Curr. Opin. Chem. Biol.* **2009**, *13*, 678.
[18] J. Hemphill, E. K. Borchardt, K. Brown, A. Asokan, A. Deiters, *J. Am. Chem. Soc.* **2015**, *137*, 5642.
[19] L. R. Polstein, C. A. Gersbach, *Nat. Chem. Biol.* **2015**, *11*, 198.
[20] Y. Nihongaki, F. Kawano, T. Nakajima, M. Sato, *Nat. Biotechnol.* **2015**, *33*, 755.
[21] L. R. Polstein, C. A. Gersbach, *J. Am. Chem. Soc.* **2012**, *134*, 16480.
[22] E. J. Gomez, K. Gerhardt, J. Judd, J. J. Tabor, J. Suh, *ACS Nano* **2016**, *10*, 225.
[23] J. Hemphill, Q. Y. Liu, R. Uprety, S. Samanta, M. Tsang, R. L. Juliano, A. Deiters, *J. Am. Chem. Soc.* **2015**, *137*, 3656.
[24] V. Mikat, A. Heckel, *RNA* **2007**, *13*, 2341.
[25] C. T. Huynh, M. K. Nguyen, G. Y. Tonga, L. Longe, V. M. Rotello, E. Alsberg, *Adv. Healthcare Mater.* **2016**, *5*, 305.
[26] R. E. Kohman, S. S. Cha, H. Y. Man, X. Han, *Nano Lett.* **2016**, *16*, 2781.
[27] S. Y. Lee, Y. H. Lai, K. C. Huang, Y. H. Cheng, T. F. Tseng, C. K. Sun, *Sci. Rep.* **2015**, *5*, 15421.
[28] R. Weissleder, *Nat. Biotechnol.* **2001**, *19*, 316.
[29] B. P. Timko, D. S. Kohane, *Expert Opin. Drug Delivery* **2014**, *11*, 1681.
[30] X. Huang, A. Pallaoro, G. B. Braun, D. P. Morales, M. O. Ogunyankin, J. Zasadzinski, N. O. Reich, *Nano Lett.* **2014**, *14*, 2046.
[31] G. B. Braun, A. Pallaoro, G. Wu, D. Missirlis, J. A. Zasadzinski, M. Tirrell, N. O. Reich, *ACS Nano* **2009**, *3*, 2007.
[32] D. P. Morales, G. B. Braun, A. Pallaoro, R. Chen, X. Huang, J. A. Zasadzinski, N. O. Reich, *Mol. Pharm.* **2015**, *12*, 600.
[33] X. Huang, Q. R. Hu, G. B. Braun, A. Pallaoro, D. P. Morales, J. Zasadzinski, D. O. Clegg, N. O. Reich, *Biomaterials* **2015**, *63*, 70.
[34] E. Y. Lukianova-Hleb, A. Belyanin, S. Kashinath, X. Wu, D. O. Lapotko, *Biomaterials* **2012**, *33*, 1821.
[35] Y. Lei, D. V. Schaffer, *Proc. Natl. Acad. Sci. USA* **2013**, *110*, E5039.
[36] S. Javaherian, N. Anesiadis, R. Mahadevan, A. P. McGuigan, *Integr. Biol.* **2013**, *5*, 578.
[37] D. A. De Ugarte, K. Morizono, A. Elbarbary, Z. Alfonso, P. A. Zuk, M. Zhu, J. L. Dragoo, P. Ashjian, B. Thomas, P. Benhaim, I. Chen, J. Fraser, M. H. Hedrick, *Cells Tissues Organs* **2003**, *174*, 101.
[38] J. Gilleron, W. Querbes, A. Zeigerer, A. Borodovsky, G. Marsico, U. Schubert, K. Manygoats, S. Seifert, C. Andree, M. Stoter, H. Epstein-Barash, L. G. Zhang, V. Koteliansky, K. Fitzgerald, E. Fava, M. Bickle, Y. Kalaidzidis, A. Akinc, M. Maier, M. Zerial, *Nat. Biotechnol.* **2013**, *31*, 638.
[39] C. D. Austin, X. H. Wen, L. Gazzard, C. Nelson, R. H. Scheller, S. J. Scales, *Proc. Natl. Acad. Sci. USA* **2005**, *102*, 17987.
[40] Y. Sasai, *Nature* **2013**, *493*, 318.
[41] C. M. Pineda, S. Park, K. R. Mesa, M. Wolfel, D. G. Gonzalez, A. M. Haberman, P. Rompolas, V. Greco, *Nat. Protoc.* **2015**, *10*, 1116.